

# Research Update CHAIN ANALYSIS

Anthony Medrano

February 9, 2017

## 1 Observations of Chains

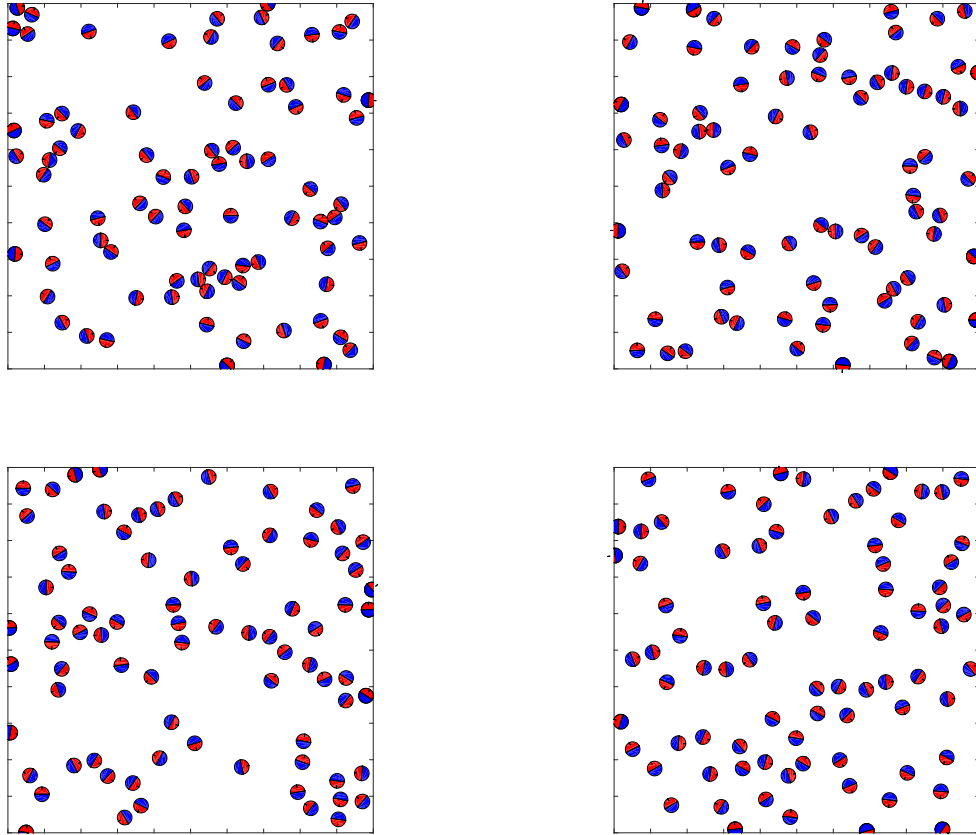


Figure 1: The area fraction  $\Phi_A$  is 0.1 and the rotational mobility coefficient  $\nu$  takes the values 1, 10, 100 and 1000 from left to right, top to bottom.

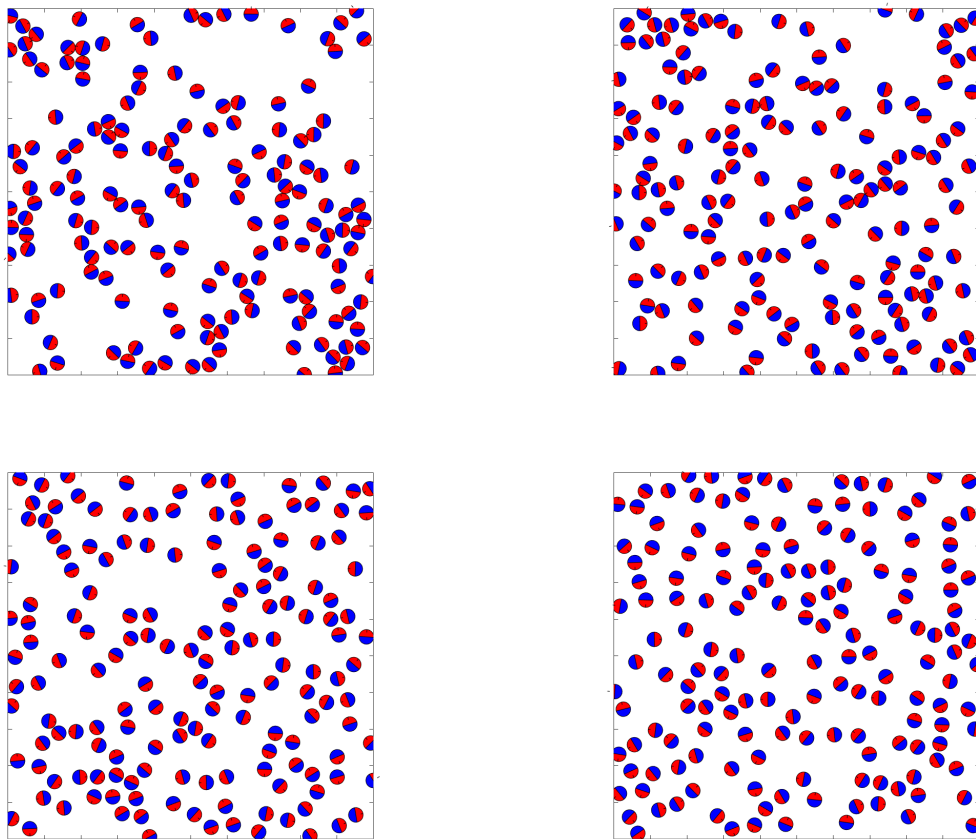


Figure 2: The area fraction  $\Phi_A$  is 0.2 and the rotational mobility coefficient  $\nu$  takes the values 1, 10, 100 and 1000 from left to right, top to bottom.

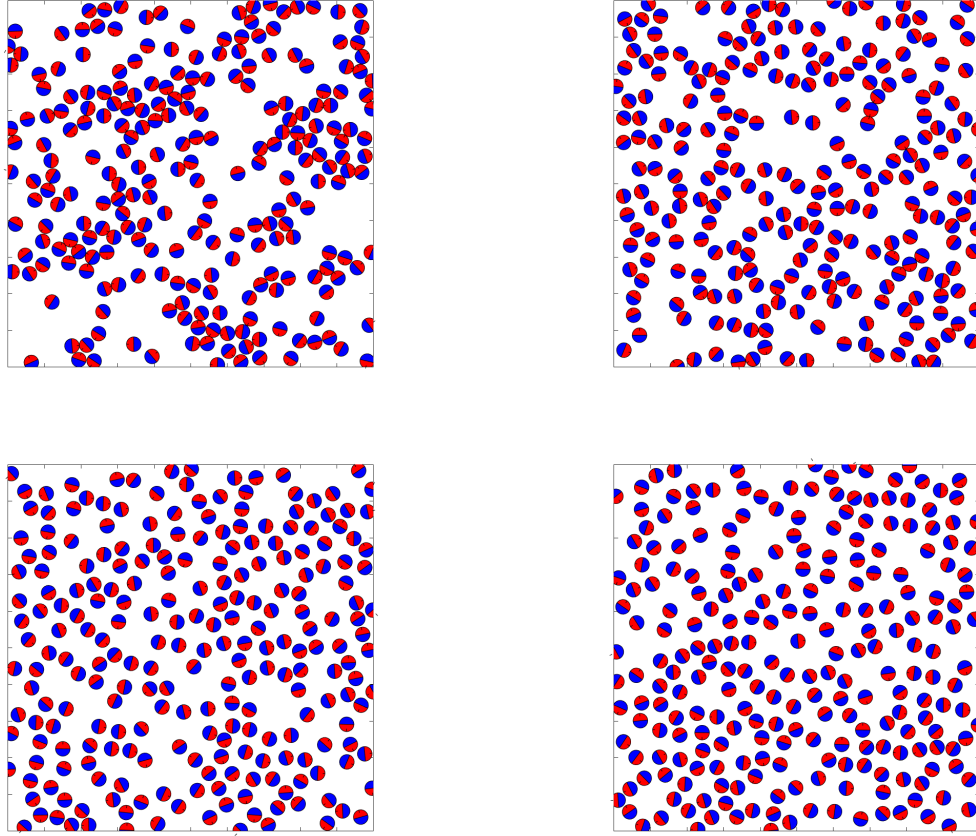


Figure 3: The area fraction  $\Phi_A$  is 0.3 and the rotational mobility coefficient  $\nu$  takes the values 1, 10, 100 and 1000 from left to right, top to bottom.

## 2 Qualitative Description

It is clear from Figures (1-3) that as  $\nu$  increases the Janus particles transition from a clumped, non-homogeneous spatial distribution to a more orderly, homogeneous one. The presence of chains becomes apparent around  $\nu = 10$  and is pronounced when  $\nu$  is greater than or equal to 100. The chains are sensitive to neighboring particles so they do not last on average more than a few time units. However, at larger values of  $\nu$  they are more quick to regroup and form new chains. The length of the chains and persistence time both increase when  $\nu$  increases. Below is a table depicting the values of  $\nu$  when chains are observed.

$\nu$	<b>1</b>	<b>10</b>	<b>100</b>	<b>1000</b>
<i>Chains</i>	no	yes	yes	yes

## 3 Correlation Metrics for Velocity and Orientation

In order to quantify the correlation in translation and orientation in the observed chains, we turn to vector projection which takes the form

$$\cos(\theta) = \frac{\mathbf{\hat{r}}_1 \cdot \mathbf{\hat{r}}_2}{|\mathbf{\hat{r}}_1| |\mathbf{\hat{r}}_2|} \quad (1)$$

where  $\mathbf{\hat{r}}_1$  and  $\mathbf{\hat{r}}_2$  are the tangential velocity vectors of two particles and  $\theta$  is the difference between their orientations. The orientations and translations of a population of Janus particles is dictated by different

but linked governing equations. For quantifiable measurements of chain formation, we seek to reformulate Equation (1) to satisfy three different local areas of interest: an ellipse with major axis parallel to the particle's orientation  $\mathbf{p}$ , an ellipse with major axis perpendicular to the particle's orientation, and a circle, as shown in Figure (4). For the ellipses, the semi-minor axis was set to 1 diameter and the semi-major axis varies from 1 diameter to 3 diameters. The radius of the circle varies from 1 diameter to 3 diameters. For

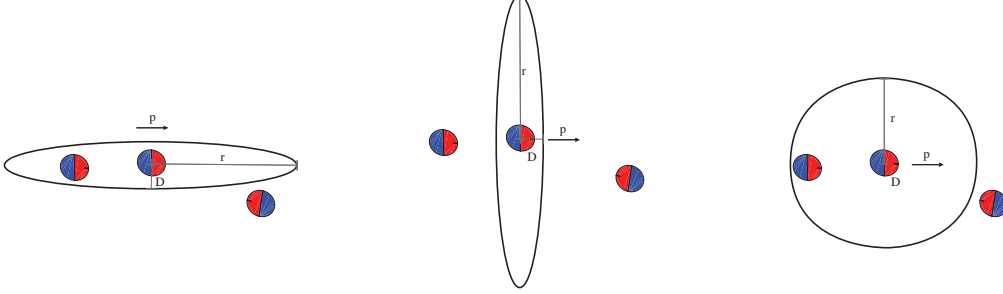


Figure 4: *Schematics of correlation zones.*

independent correlations in velocity and orientation, we separate both sides of Equation (1) and for the circle the equations take the form

$$C_v(r) = \frac{1}{Nt_f} \int_0^{t_f} \sum_{i=1}^N \sum_{j \neq i}^N \frac{\dot{\mathbf{r}}_i(t) \cdot \dot{\mathbf{r}}_j(t)}{|\dot{\mathbf{r}}_i(t)|^2} \delta [\Theta (|\mathbf{r}_i(t) - \mathbf{r}_j(t)| - r)] dt \quad (2)$$

$$C_\theta(r) = \frac{1}{Nt_f} \int_0^{t_f} \sum_{i=1}^N \sum_{j \neq i}^N \cos(\alpha_i(t) - \alpha_j(t)) \delta [\Theta (|\mathbf{r}_i(t) - \mathbf{r}_j(t)| - r)] dt \quad (3)$$

respectively. Each correlation value will approach unity the greater the correlation between particles. Correlation values near unity indicate the presence of chains but also similarity between correlation values indicates the individual particles are more closely resembling a unified system. In the limit as the changes in orientation and velocities among particles of a chain approach zero, both correlation values are equivalent to each other and satisfy Equation (1).

## 4 Spatial Correlations

For the following set of plots, the values of  $C_v$  and  $C_\theta$  were averaged over a simulation period of 500 time units.

## 4.1 Absence of Chains

### 4.1.1 $\Phi_A = 0.1$ $\nu = 1$

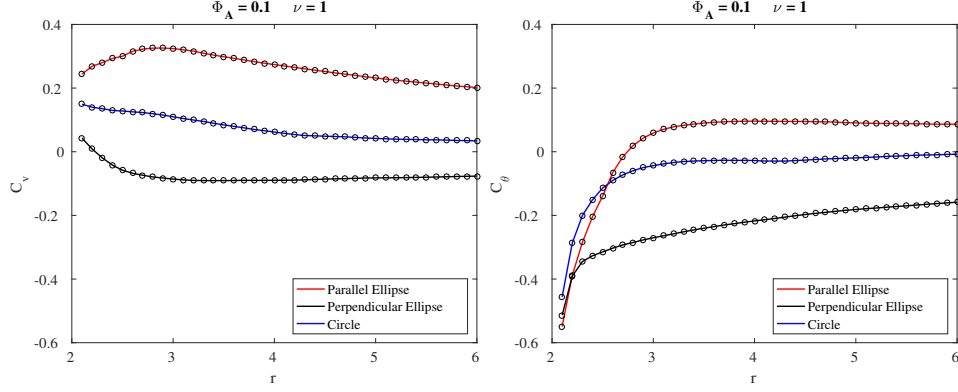


Figure 5: For the ellipses, the semi-minor axis is fixed at 1D while the semi-major axis varies from 1D( $r = 2$ ) to 3D( $r = 6$ ). Therefore the aspect ratio varies from 1 to 3. For the circle,  $r$  refers to its radius.

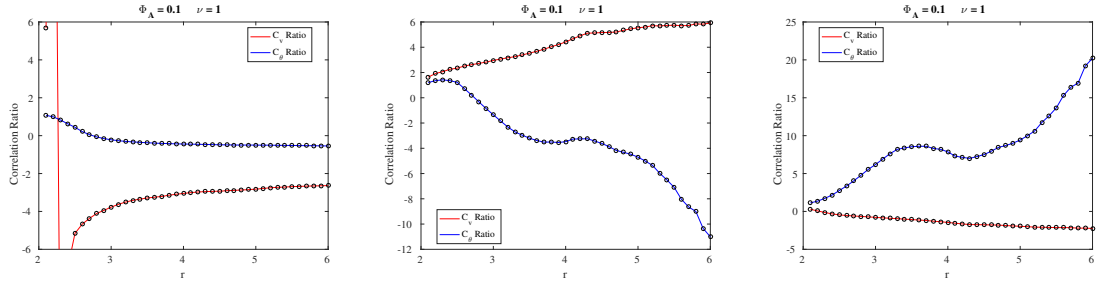


Figure 6: From left to right, the subfigures represent the ratio of correlation values between the parallel ellipse and perpendicular ellipse, the parallel ellipse and circle, and the perpendicular ellipse and circle.

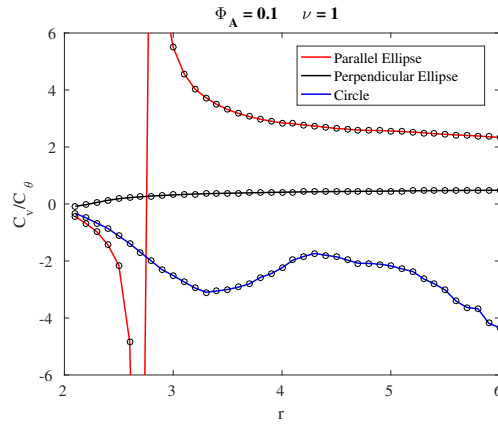


Figure 7: Ratios of velocity to orientation correlation values for each correlation zone.

#### 4.1.2 $\Phi_A = 0.2$ $\nu = 1$

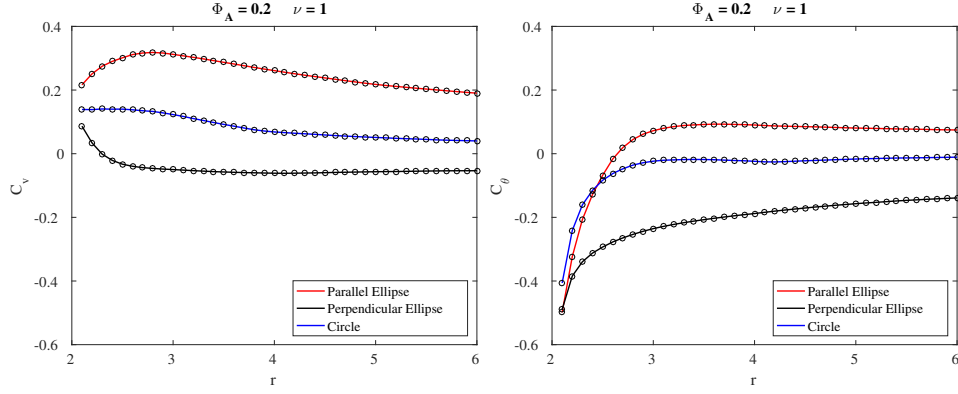


Figure 8: For the ellipses, the semi-minor axis is fixed at  $1D$  while the semi-major axis varies from  $1D(r=2)$  to  $3D(r=6)$ . Therefore the aspect ratio varies from 1 to 3. For the circle,  $r$  refers to its radius.

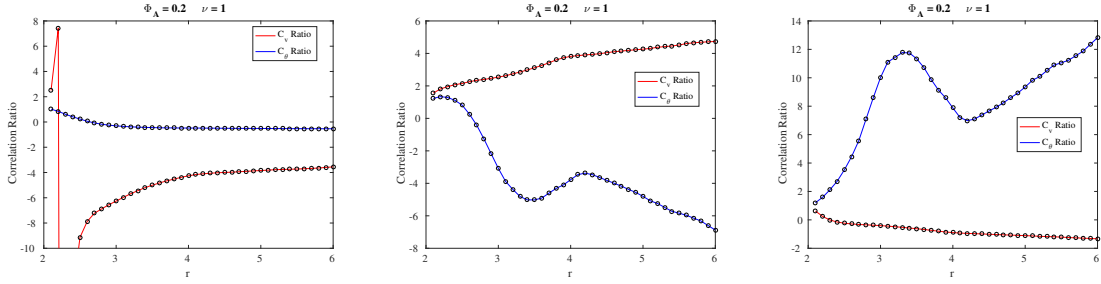


Figure 9: From left to right, the subfigures represent the ratio of correlation values between the parallel ellipse and perpendicular ellipse, the parallel ellipse and circle, and the perpendicular ellipse and circle.

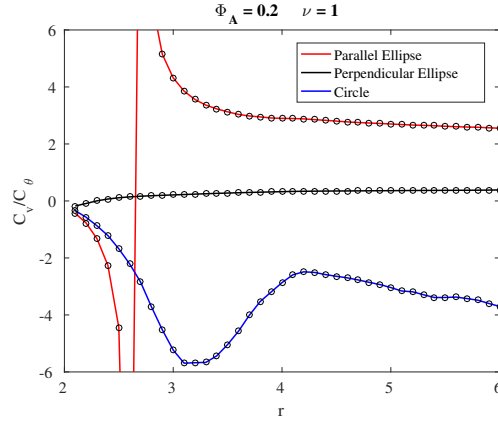


Figure 10: Ratios of velocity to orientation correlation values for each correlation zone.

#### 4.1.3 $\Phi_A = 0.3$ $\nu = 1$

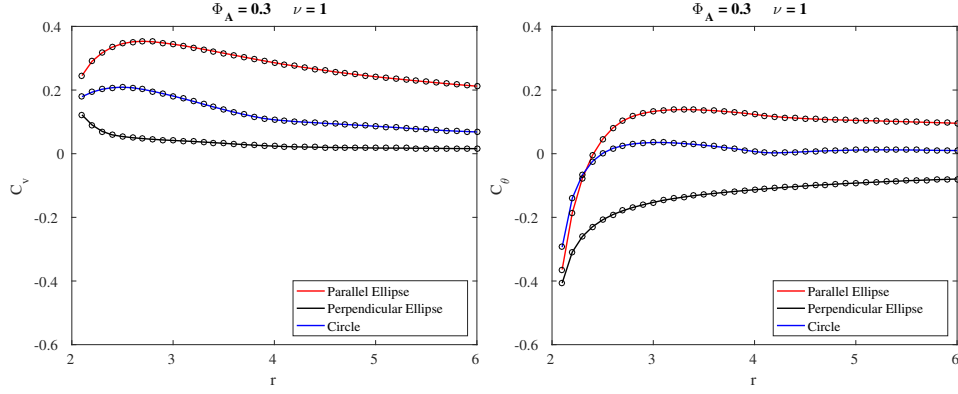


Figure 11: For the ellipses, the semi-minor axis is fixed at  $1D$  while the semi-major axis varies from  $1D(r=2)$  to  $3D(r=6)$ . Therefore the aspect ratio varies from 1 to 3. For the circle,  $r$  refers to its radius.

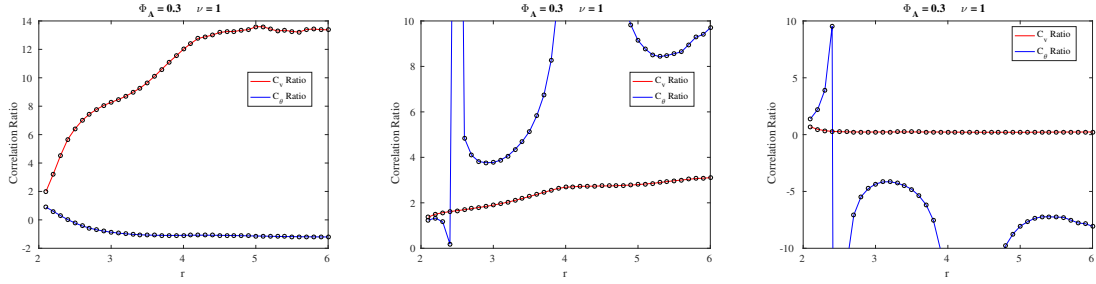


Figure 12: From left to right, the subfigures represent the ratio of correlation values between the parallel ellipse and perpendicular ellipse, the parallel ellipse and circle, and the perpendicular ellipse and circle.

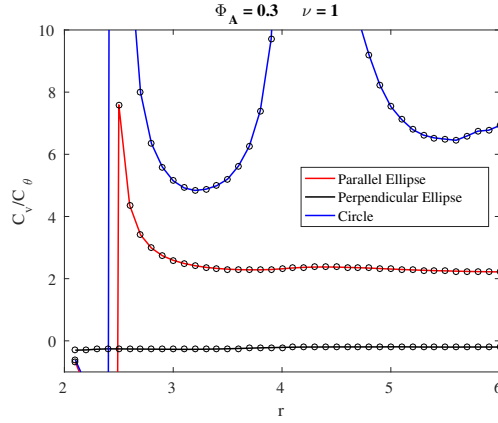


Figure 13: Ratios of velocity to orientation correlation values for each correlation zone.

## 4.2 Presence of Chains

### 4.2.1 $\Phi_A = 0.1$ $\nu = 1000$

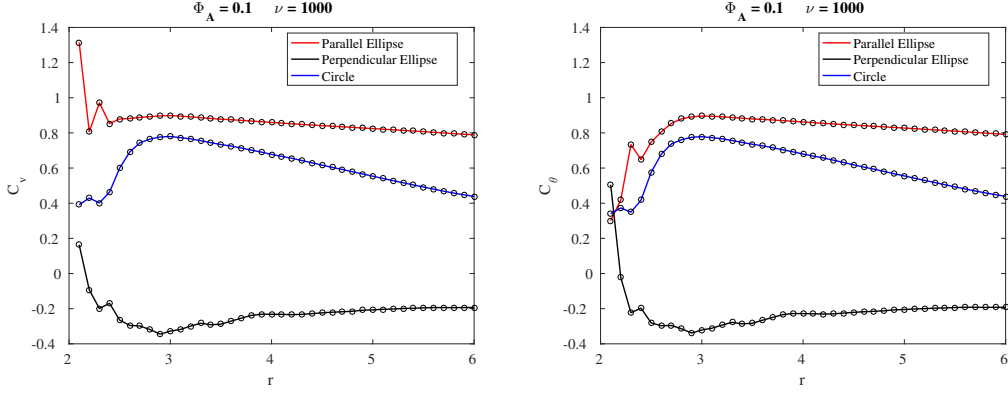


Figure 14: For the ellipses, the semi-minor axis is fixed at  $1D$  while the semi-major axis varies from  $1D(r=2)$  to  $3D(r=6)$ . Therefore the aspect ratio varies from 1 to 3. For the circle,  $r$  refers to its radius.

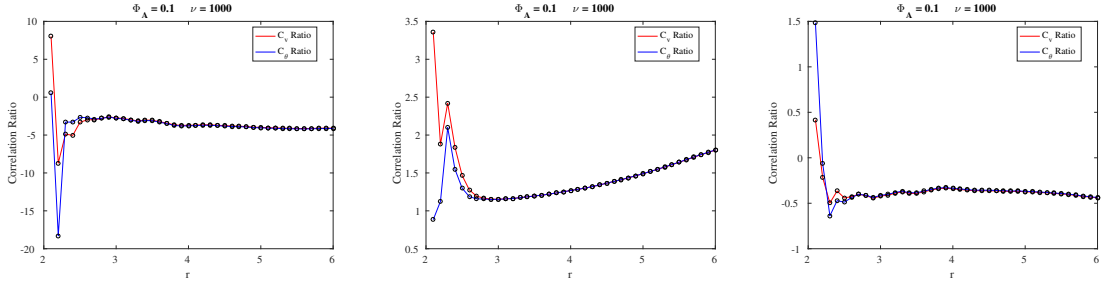


Figure 15: From left to right, the subfigures represent the ratio of correlation values between the parallel ellipse and perpendicular ellipse, the parallel ellipse and circle, and the perpendicular ellipse and circle.

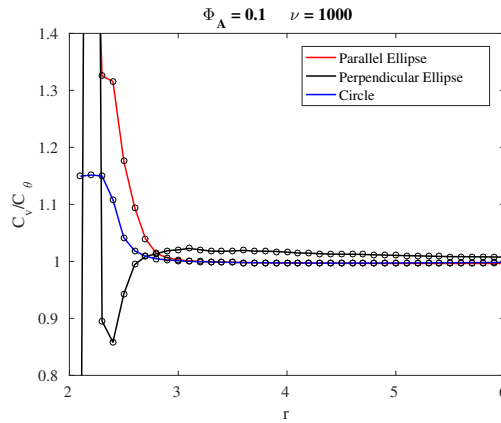


Figure 16: Ratios of velocity to orientation correlation values for each correlation zone.



#### 4.2.2 $\Phi_A = 0.2$ $\nu = 1000$

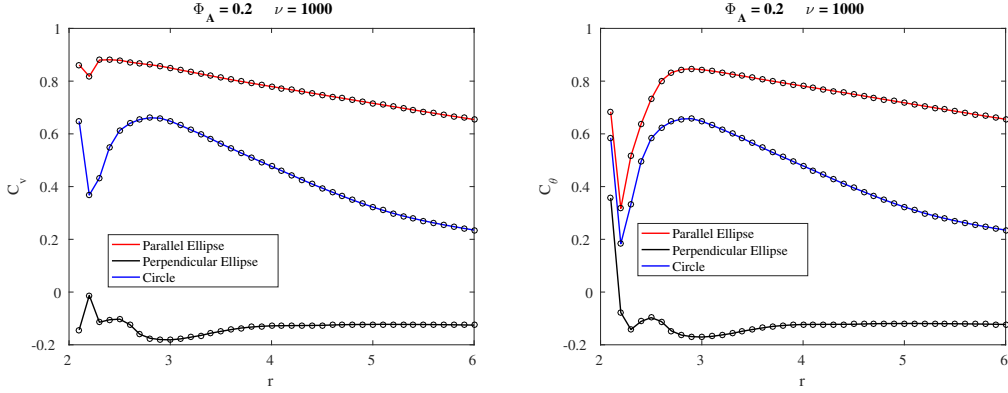


Figure 17: For the ellipses, the semi-minor axis is fixed at  $1D$  while the semi-major axis varies from  $1D$  ( $r = 2$ ) to  $3D$  ( $r = 6$ ). Therefore the aspect ratio varies from 1 to 3. For the circle,  $r$  refers to its radius.

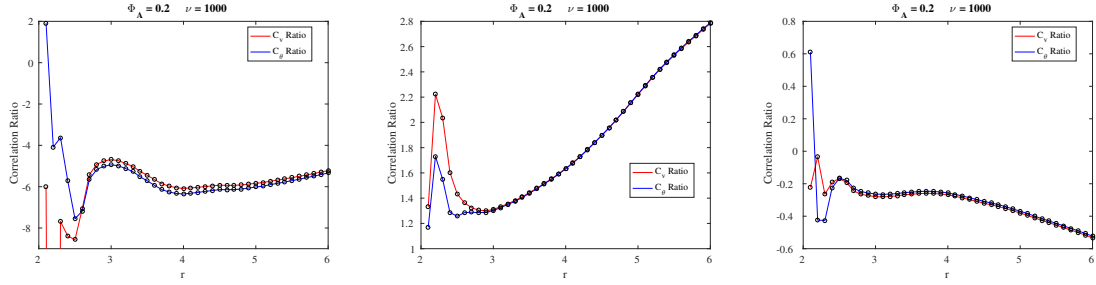


Figure 18: From left to right, the subfigures represent the ratio of correlation values between the parallel ellipse and perpendicular ellipse, the parallel ellipse and circle, and the perpendicular ellipse and circle.

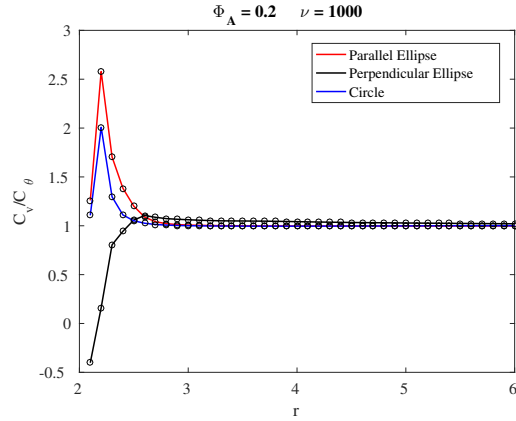


Figure 19: Ratios of velocity to orientation correlation values for each correlation zone.

#### 4.2.3 $\Phi_A = 0.3 \quad \nu = 1000$

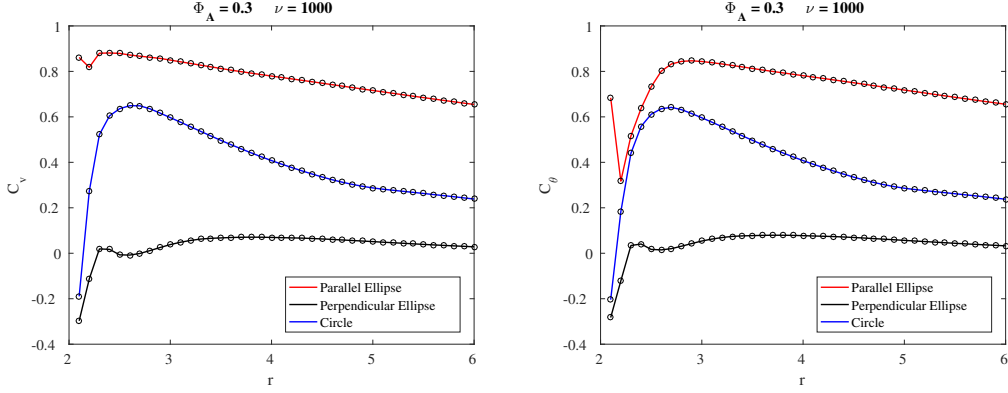


Figure 20: For the ellipses, the semi-minor axis is fixed at  $1D$  while the semi-major axis varies from  $1D$  ( $r = 2$ ) to  $3D$  ( $r = 6$ ). Therefore the aspect ratio varies from 1 to 3. For the circle,  $r$  refers to its radius.

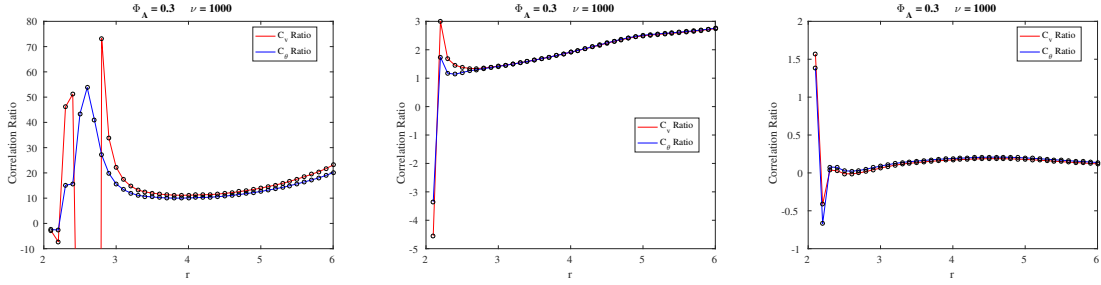


Figure 21: From left to right, the subfigures represent the ratio of correlation values between the parallel ellipse and perpendicular ellipse, the parallel ellipse and circle, and the perpendicular ellipse and circle.

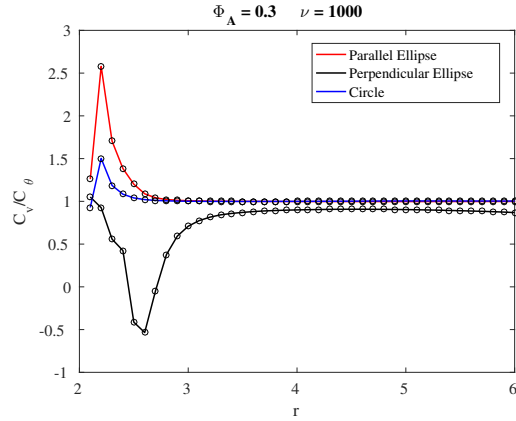


Figure 22: Ratios of velocity to orientation correlation values for each correlation zone.

## 5 Temporal Correlations

For the temporal correlation plots, the correlation values were averaged over periods of  $3D/U$  where  $D$  is the diameter of a particle and  $U$  is the self-propelled velocity. For the time scale, a distance of  $3D$  was chosen because the amplitude of the dipolar field surrounding a particle is approximately 3% of the value at its boundary. We assume the effects a particle has on its neighbor past that distance is negligible.

## 5.1 Absence of Chains

### 5.1.1 $\Phi_A = 0.1$ $\nu = 1$

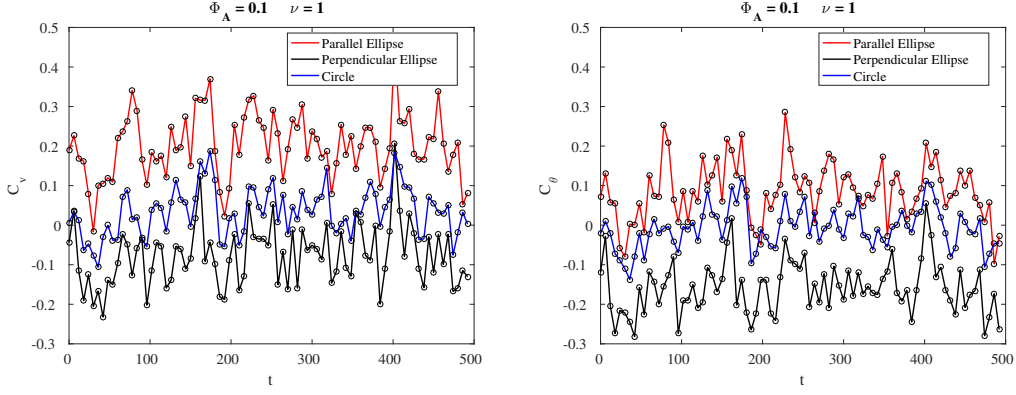


Figure 23: For the ellipses the semi-major axis is  $r = 3D$  and the semi-minor axis is  $1D$  hence the aspect ratio is 3. For the circle, the radius is fixed at  $3D$ .

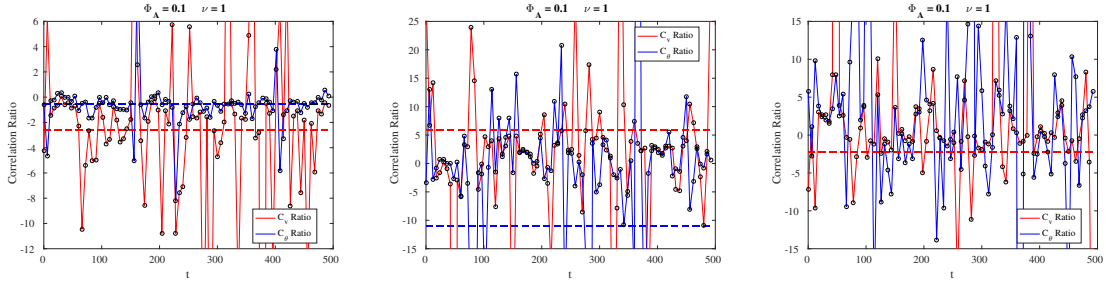


Figure 24: From left to right, the subfigures represent the ratio of correlation values between the parallel ellipse and perpendicular ellipse, the parallel ellipse and circle, and the perpendicular ellipse and circle. The colored dashed lines are the ratios of the respective color's averaged correlation values.

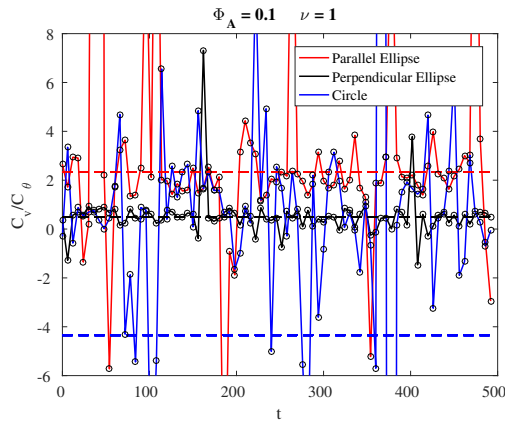


Figure 25: Ratios of velocity to orientation correlation values for each correlation zone. The colored dashed lines are the ratios of the respective color's averaged correlation values.

### 5.1.2 $\Phi_A = 0.2$ $\nu = 1$

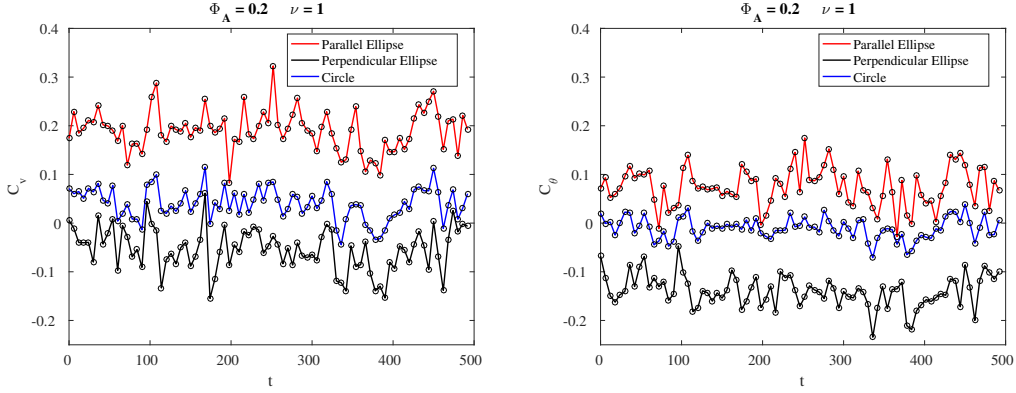


Figure 26: The semi-major axis is  $r = 3D$  and the semi-minor axis is  $1D$  hence the aspect ratio is 3. For the circle, the radius is fixed at  $3D$ .

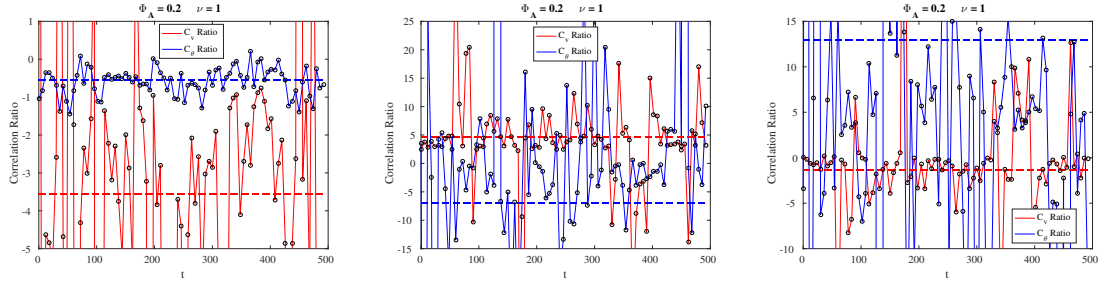


Figure 27: From left to right, the subfigures represent the ratio of correlation values between the parallel ellipse and perpendicular ellipse, the parallel ellipse and circle, and the perpendicular ellipse and circle. The colored dashed lines are the ratios of the respective color's averaged correlation values.

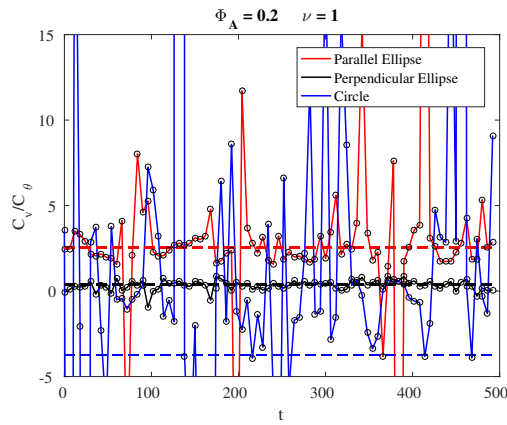


Figure 28: Ratios of velocity to orientation correlation values for each correlation zone. The colored dashed lines are the ratios of the respective color's averaged correlation values.

### 5.1.3 $\Phi_A = 0.3 \ \nu = 1$

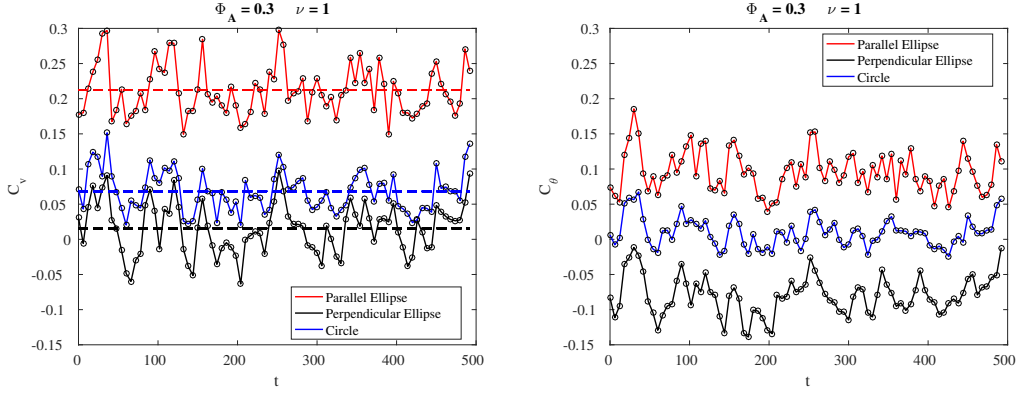


Figure 29: The semi-major axis is  $r = 3D$  and the semi-minor axis is  $1D$  hence the aspect ratio is 3. For the circle, the radius is fixed at  $3D$ .

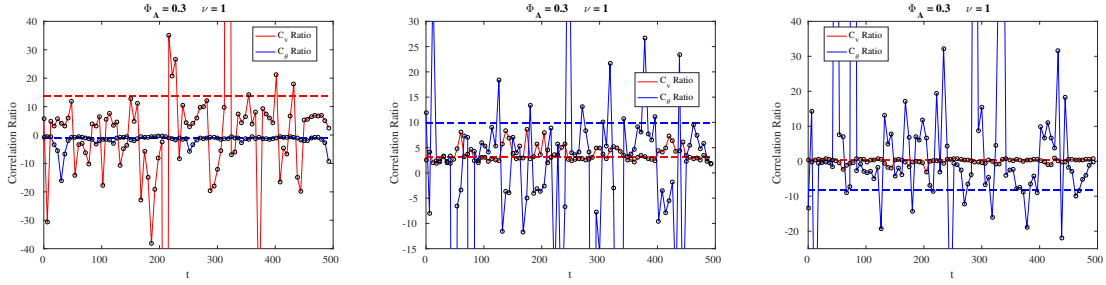


Figure 30: From left to right, the subfigures represent the ratio of correlation values between the parallel ellipse and perpendicular ellipse, the parallel ellipse and circle, and the perpendicular ellipse and circle. The colored dashed lines are the ratios of the respective color's averaged correlation values.

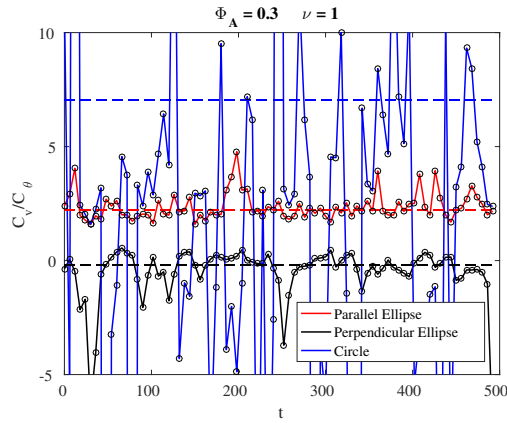


Figure 31: Ratios of velocity to orientation correlation values for each correlation zone. The colored dashed lines are the ratios of the respective color's averaged correlation values.

## 5.2 Presence of Chains

### 5.2.1 $\Phi_A = 0.1$ $\nu = 1000$

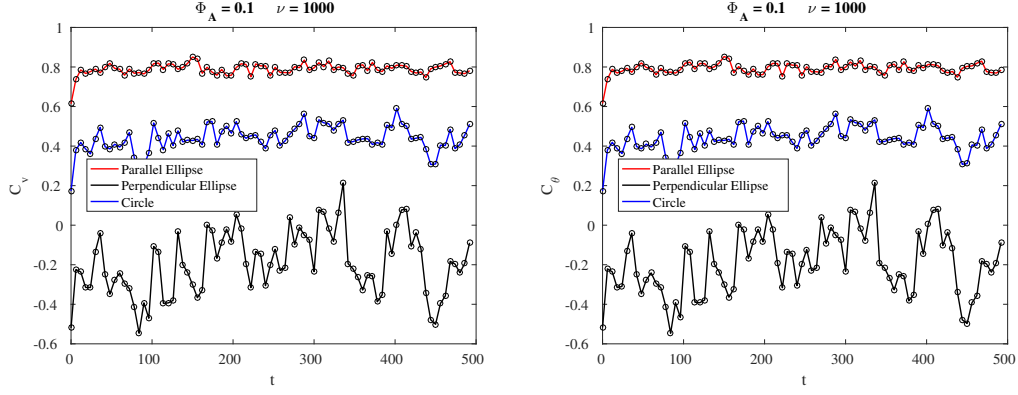


Figure 32: The semi-major axis is  $r = 3D$  and the semi-minor axis is  $1D$  hence the aspect ratio is 3. For the circle, the radius is fixed at  $3D$ .

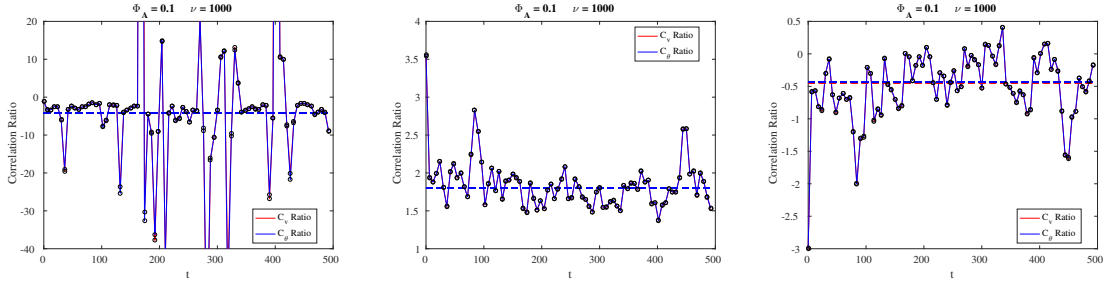


Figure 33: From left to right, the subfigures represent the ratio of correlation values between the parallel ellipse and perpendicular ellipse, the parallel ellipse and circle, and the perpendicular ellipse and circle. The colored dashed lines are the ratios of the respective color's averaged correlation values.

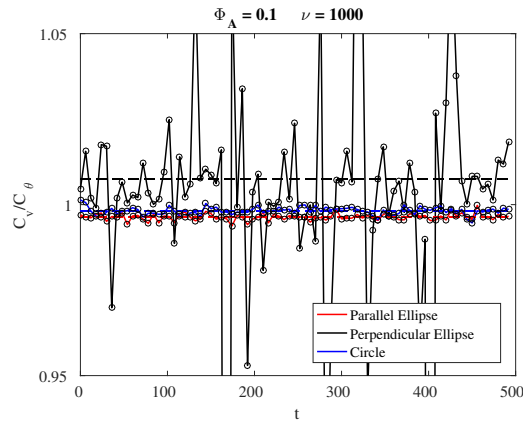


Figure 34: Ratios of velocity to orientation correlation values for each correlation zone. The colored dashed lines are the ratios of the respective color's averaged correlation values.

### 5.2.2 $\Phi_A = 0.2 \quad \nu = 1000$

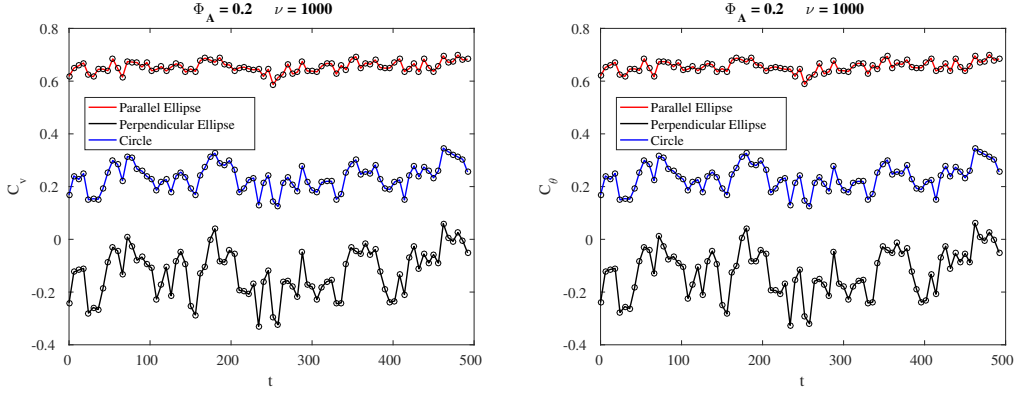


Figure 35: The semi-major axis is  $r = 3D$  and the semi-minor axis is  $1D$  hence the aspect ratio is 3. For the circle, the radius is fixed at  $3D$ .

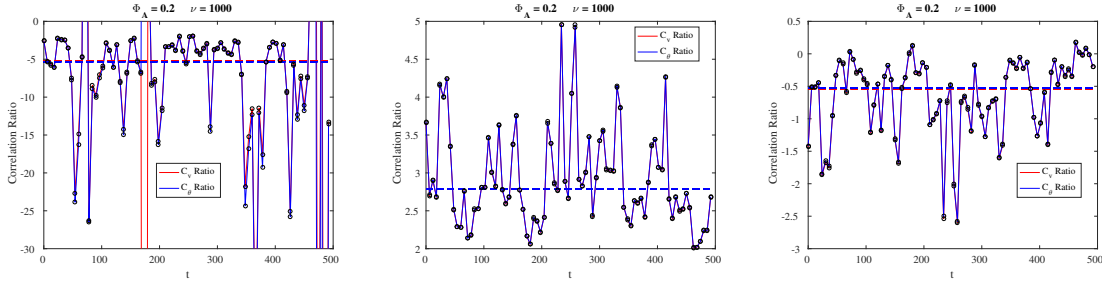


Figure 36: From left to right, the subfigures represent the ratio of correlation values between the parallel ellipse and perpendicular ellipse, the parallel ellipse and circle, and the perpendicular ellipse and circle. The colored dashed lines are the ratios of the respective color's averaged correlation values.

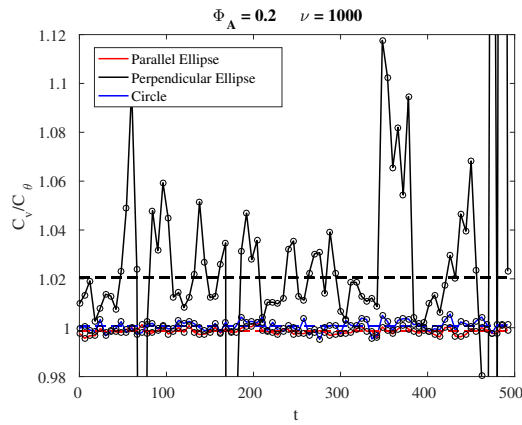


Figure 37: Ratios of velocity to orientation correlation values for each correlation zone. The colored dashed lines are the ratios of the respective color's averaged correlation values.



### 5.2.3 $\Phi_A = 0.3$ $\nu = 1000$

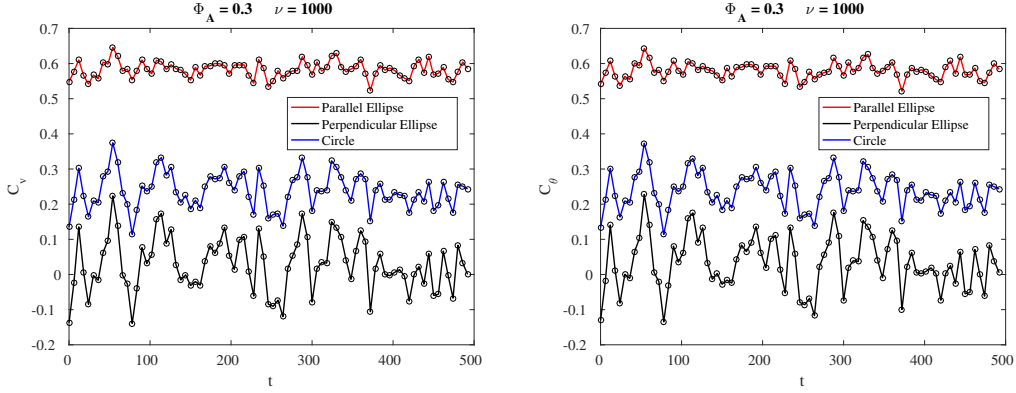


Figure 38: The semi-major axis is  $r = 3D$  and the semi-minor axis is  $1D$  hence the aspect ratio is 3. For the circle, the radius is fixed at  $3D$ .

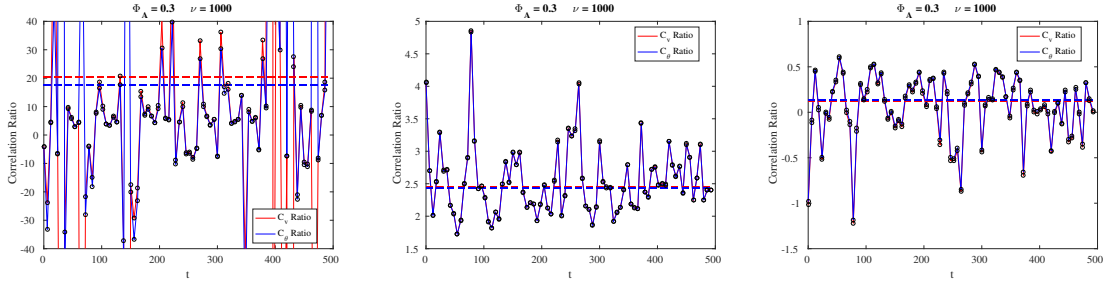


Figure 39: From left to right, the subfigures represent the ratio of correlation values between the parallel ellipse and perpendicular ellipse, the parallel ellipse and circle, and the perpendicular ellipse and circle. The colored dashed lines are the ratios of the respective color's averaged correlation values.

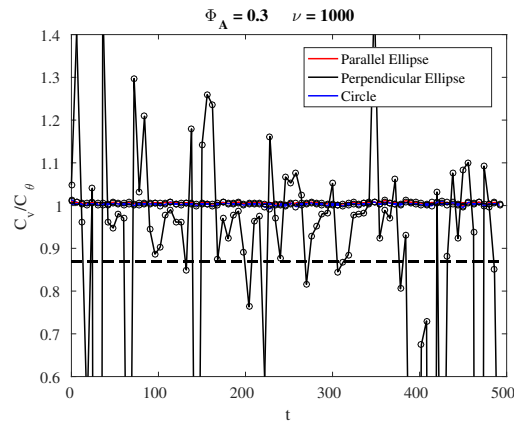


Figure 40: Ratios of velocity to orientation correlation values for each correlation zone. The colored dashed lines are the ratios of the respective color's averaged correlation values.

## 6 Summary

The spatially dependent correlation values at  $\nu = 1$  were closer to zero than one across three area fractions, signaling the absence of chains. Furthermore, it is clear from observation that the values for both values were different, thereby suggesting a disorderly system of particles. In contrast, the correlation values at  $\nu = 1000$  were greater in magnitude than their counterparts. For  $\nu = 1000$ , the highest correlation values occurred at the lowest area fraction. In the case of the circle and parallel ellipse zones, the correlation values were much closer to unity, especially for the ellipse. The results also supported intuition that an ellipse parallel to a particle's orientation would generate the greatest correlation in a dipolar flow. The ellipse perpendicular to orientation naturally produced the lowest values of the three correlation zones. Negative correlation values for an area defined by a perpendicular ellipse is explained by the tendency of particles to align opposite to their neighbor's chemical gradient, which has a sink in the front and a source at the end. The separation region with greatest correlation values was around  $2.5r$  to  $r$  which lies just outside the steric dominant zone.

The temporally dependent correlation values at  $\nu = 1$  tended to show more fluctuations on average than that of  $\nu = 1000$ . This indicates that the order of the system is more stable at higher  $\nu$  values, which is consistent with a strong presence of chains and order. However, the opposite is true for the perpendicular ellipse correlation zone. For  $\nu = 1000$ , the highest correlation values occurred at the lowest area fraction. Like the spatially dependent correlation values, the similarity between both temporally dependent correlation values occurred at higher  $\nu$ .

Furthermore, the similarity or difference between spatially dependent correlation values can be quantified by taking the absolute difference between them at each distance. For temporally dependent correlation values the mean and standard deviation of both time series can be compared.

## 7 Revised Spatial Correlations

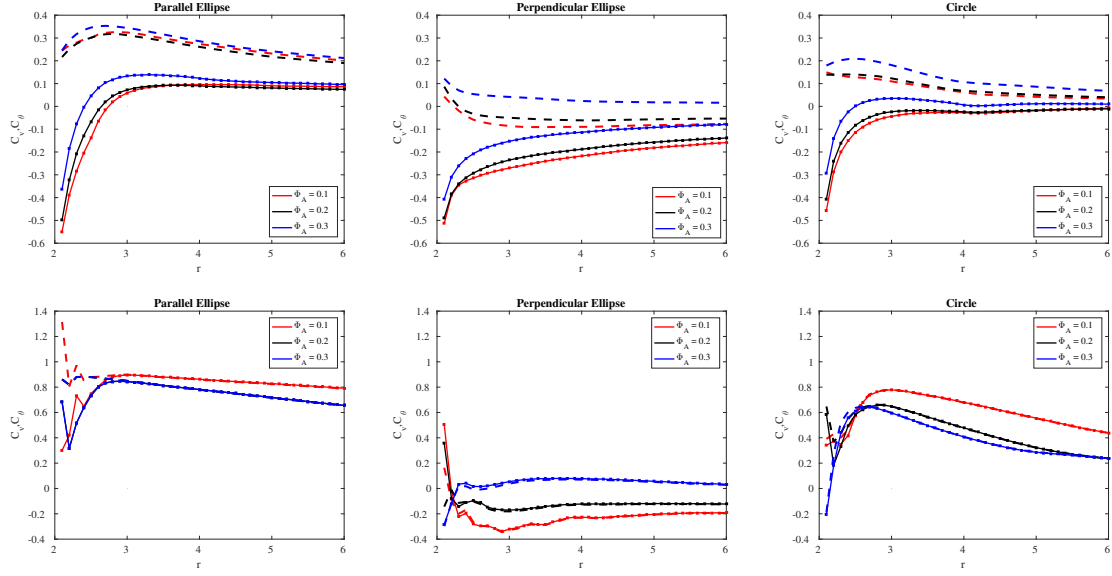


Figure 41: The top row of plots represent a population where no chains are present ( $\nu = 1$ ) and the bottom row represents a population where chains are present ( $\nu = 1000$ ). The dashed lines represent the correlation in velocity  $C_v$  and the solid lines with square data points represent the correlation in orientation  $C_\theta$ . There is greater disparity between the two correlations ( $C_v, C_\theta$ ) when the rotational coefficient  $\nu$  is low, as shown in the top row plots. When  $\nu$  is large (bottom row plots) the two correlation values nearly converge outside the steric dominant region ( $\sim r > 2.5$ ). For  $\nu = 1000$ , there is a clear trend outside the steric region across area fractions. The absolute value of the correlations decreases with increasing area fraction suggesting that more particles hinders the formation of chains. When  $\nu = 1$ , the correlations across area fractions sometimes overlap at seemingly arbitrary values of  $r$  and makes it difficult to observe a trend, suggesting that perhaps the collective behavior is more random. For the ellipses, the semi-minor axis is fixed at 1D while the semi-major axis varies from 1D ( $r = 2$ ) to 3D ( $r = 6$ ). Therefore the aspect ratio varies from 1 to 3. For the circle,  $r$  refers to its radius.

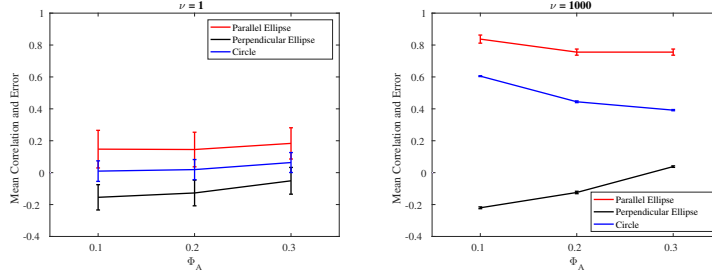


Figure 42: The correlation values  $C_v, C_\theta$  were individually averaged from  $r = 2$  to  $r = 6$  and then averaged with respect to each other, i.e.  $\langle \langle C_v \rangle, \langle C_\theta \rangle \rangle$ , for each correlation zone. They were plotted along with the absolute value of the error of the means  $|\langle C_v \rangle - \langle C_\theta \rangle|$ . The upper and lower error bars are at a distance of half the error from the mean correlation. The error is a measure of consistency for Equation (4) below where  $C_\theta$  represents the left hand side and  $C_v$  represents the right hand side. The mean correlation value,  $\langle \langle C_v \rangle, \langle C_\theta \rangle \rangle$ , is a measure of the strength of correlation between two particles. If the mean correlation value is near unity and the error is small then there are chains within the population. In the left plot where  $\nu = 1$ , the large error bars and low mean correlation indicate that the orientation and velocity between are weakly correlated. However, when  $\nu = 1000$ , the error is on the order of  $10^{-1}$  or less, which means that Equation (4) is relatively consistent. The larger error bars for the parallel elliptical zone may be attributed to the larger differences between both correlation values within the steric region as shown in the bottom left plot of Figure (41). It is apparent from the right plot that the parallel elliptical correlation zone is the most fit of the three zones for detecting the presence of chains. Also, it is apparent that the absolute value of the mean correlation decreases with increasing area fraction.

The rearranged scalar projection equation takes the form,

$$\cos(\theta) = \frac{\dot{\mathbf{r}}_1 \cdot \dot{\mathbf{r}}_2}{|\dot{\mathbf{r}}_1| |\dot{\mathbf{r}}_2|}. \quad (4)$$

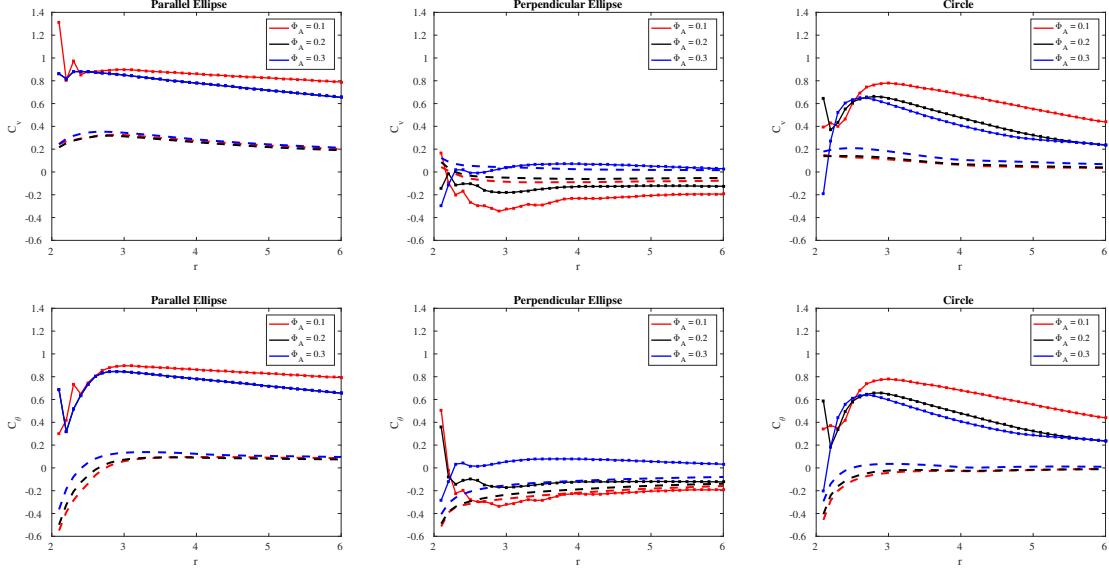


Figure 43: The dashed lines represent  $\nu = 1$  and the solid lines with square data points represent  $\nu = 1000$ . For all three correlation zones, the correlation values  $C_v, C_\theta$  for  $\nu = 1$  are close to zero and relatively constant outside the steric region ( $\sim r > 2.5$ ), indicating the absence of chains. However, for  $\nu = 1000$ , the correlation values vary significantly across correlation zones. For the parallel elliptical region, the correlation values approach unity just outside the steric region and decrease slightly in a linear fashion with increasing distance. Correlation values in the perpendicular elliptical region hover close to zero signaling lack of correlation. The circular region depicts correlation values close to unity just outside the steric region but those values decrease much more rapidly with distance than that of the parallel elliptical region. Increasing area fraction decreases correlation values. For the ellipses, the semi-minor axis is fixed at  $1D$  while the semi-major axis varies from  $1D$  ( $r = 2$ ) to  $3D$  ( $r = 6$ ). Therefore the aspect ratio varies from 1 to 3. For the circle,  $r$  refers to its radius.

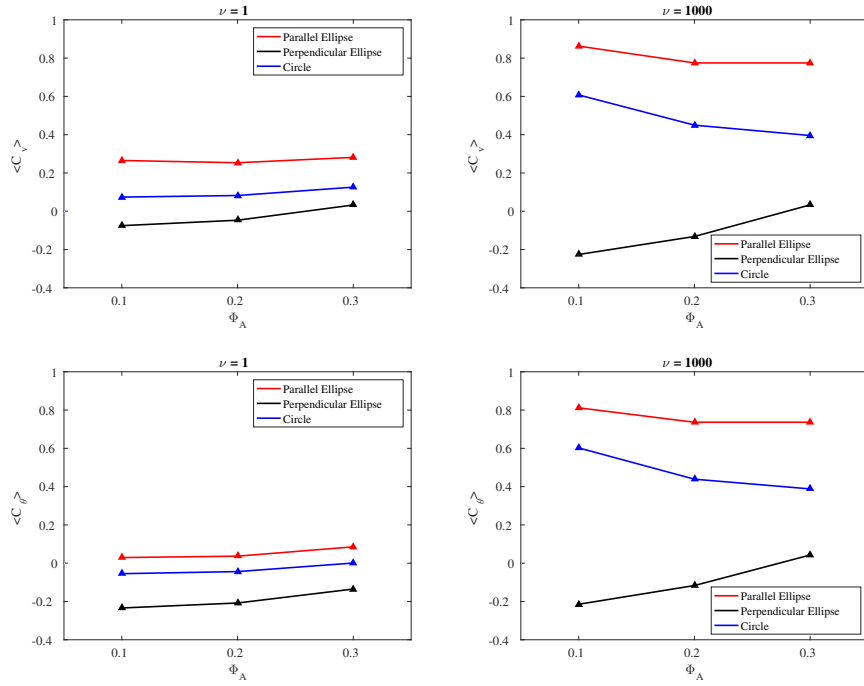


Figure 44: The correlation values  $C_v, C_\theta$  were individually averaged from  $r = 2$  to  $r = 6$  for each area fraction and correlation zone. Mean correlation values near unity indicates the presence of chains within the population. It is clear from the right plots that the parallel elliptical correlation zone is the most fit of the three zones for detecting the presence of chains. Also, it is apparent that the absolute value of the correlations decreases with increasing area fraction.